Wilfrid Laurier University

Scholars Commons @ Laurier

Physics and Computer Science Faculty Publications

Physics and Computer Science

12-1990

Polarization Characteristics of Double-Clad Elliptical Fibers

Feng Zhang
University of Waterloo

John W.Y. Lit
Wilfrid Laurier University, jlit@wlu.ca

Follow this and additional works at: https://scholars.wlu.ca/phys_faculty

Recommended Citation

Polarization characteristics of double-clad elliptical fibers

Feng Zhang and John W. Y. Lit

A scalar variational analysis based on a Gaussian approximation of the fundamental mode of a double-clad elliptical fiber with a depressed inner cladding is studied. The polarization properties and graphic results are presented; they are given in terms of three parameters: the ratio of the major axis to the minor axis of the core, the ratio of the inner cladding major axis to the core major axis, and the difference between the core index and the inner cladding index. The variations of both the spot size and the field intensity with core ellipticity are examined. It is shown that high birefringence and dispersion-free orthogonal polarization modes can be obtained within the single-mode region and that the field intensity distribution may be more confined to the fiber center than in a single-clad elliptical fiber.

I. Introduction

Recent progress in fiber technology by using phase or polarization modulation has given rise to new systems not only in optical communications but also in fiber sensors and in integrated optics. The ability to control and to maintain the polarization states is important in many systems, such as coherent communication systems and interferometric and polarimetric fiber sensors. The key to acquire such ability is to use high performance single-mode polarization-maintaining fibers and components. A highly birefringent fiber, in which the polarization state of the input light is preserved by minimizing the coupling between the two orthogonally polarized fundamental modes, is one of the most popular polarization-maintaining fibers. Such a fiber can be made by introducing transverse geometric asymmetry to the fiber core[1-6] or by building in transverse asymmetric stresses in the region surrounding the core.[7-10] Stress-induced birefringent fibers require manufacturing trade-offs between polarization holding and attenuation.[11] The most serious problem with these fibers, however, is that the stresses induced by different thermal expansions make polarization holding sensitive to temperature variations and restrict their practical uses.[12-14] In addition, accessing the guiding region of the fiber is a complex operation which changes the internal stresses; this adversely affects the use of the fiber to make polarization-maintaining or polarization-controlling components, such as couplers, polarizers, etc. On the other hand, if birefringence is caused by fiber geometry, bending and temperature could change over wide ranges without significantly degrading the optical performance. Such a fiber also allows easy access to the guiding region, which could be achieved by various methods such as etching and polishing, without adversely affecting the performance. Among fibers of this type, single-clad elliptical (SCE) fiber has emerged as the most practical one. It has been studied both theoretically[1,2,15,16] and experimentally.[4] The birefringence of such a fiber can be increased by increasing the ellipticity of the core or the index difference between the core and the cladding. To produce high birefringence, both the core ellipticity and the index difference have to be large, resulting in the core size being very small for a single-mode fiber.[2] This does not only make fabrication and connection more difficult, but it also enhances the nonlinear effects in the core.

To overcome these disadvantages, depressed inner cladding elliptical (DICE) fibers with self-locating D-shape have been fabricated.[17] The polarization-maintaining characteristics of DICE fibers have been investigated experimentally.[18] Theoretically they have been analyzed by means of a double-clad rectangular waveguide (DCRW) model.[19] The results show that DICE fibers, compared with SCE fibers, have higher birefringence in the weakly guiding region, zero polarization-mode dispersion in the single-mode region, and larger first-higher-mode cutoff frequency, leading to a larger core size for single-mode operation. Both the

beat length and the cutoff wavelength can be predicted reasonably well.[18] But the model cannot give the mode field distribution and spot size, which are essential to the proper design of experiments, connections, and fabrication of components.

In this paper we use the Gaussian approximation to calculate the spot size, the field distribution, the birefringence, and the polarization-mode dispersion in weakly guiding DICE fibers. We examine the effects of a depressed inner cladding and core ellipticity on these quantities.

II. Gaussian Approximation for DICE Fibers

We studied the structure shown in Fig. 1. A DICE fiber has the following parameters: a_1 and a_2 are the major axes of the core and of the inner cladding; b_1 and b_2 are the minor axes of the core and of the inner cladding; n_0, n_1, and n_2 are the refractive indices of the core, inner and outer cladding respectively. In terms of elliptical coordinates ξ and η, the two boundaries of the inner cladding may be expressed by $\xi = \xi_1$ and $\xi = \xi_2$.

The refractive index distribution in a DICE fiber can be written as (see Fig. 1)

$$n^2(\xi) = n_0^2[1 - 2\Delta_2 f(\xi)], \tag{1}$$

where

$$f(\xi) = \begin{cases} 0 & \xi < \xi_1, \\ \alpha H(\xi - \xi_1), & \xi_1 \leq \xi < \xi_2, \\ H(\xi - \xi_2), & \xi \geq \xi_2, \end{cases} \tag{2}$$

$$H(x) = \begin{cases} 0, & x < 0, \\ 1, & x \geq 0, \end{cases} \tag{3}$$

$$\alpha = \frac{\Delta_1}{\Delta_2} = \frac{n_0^2 - n_1^2}{n_0^2 - n_2^2},$$

with

$$\Delta_1 = \frac{n_0^2 - n_1^2}{2n_0^2}, \quad \Delta_2 = \frac{n_0^2 - n_2^2}{2n_0^2}. \tag{4}$$

We also introduce the parameters

$$R_x = \frac{a_2}{a_1}, \quad R_y = \frac{b_2}{b_1}.$$

If $\Delta_1 = 0$ or $= \Delta_2$ and $R_x = R_y = 1$, a double-clad elliptical fiber becomes a single-clad circular fiber. The normalized frequencies can be defined as

$$V_x = k a_1 n_0 (2\Delta_2)^{1/2}, \tag{5}$$

$$V_y = k b_1 n_0 (2\Delta_2)^{1/2}. \tag{6}$$

The fundamental modes of a weakly guiding elliptical fiber are plane polarized parallel to the major and minor axes of the ellipse. The transverse fields have the forms

$$E_x = \Psi(x,y) \exp[i(\beta + \delta\beta_x)z], \tag{7}$$

$$E_y = \Psi(x,y) \exp[i(\beta + \delta\beta_y)z]. \tag{8}$$
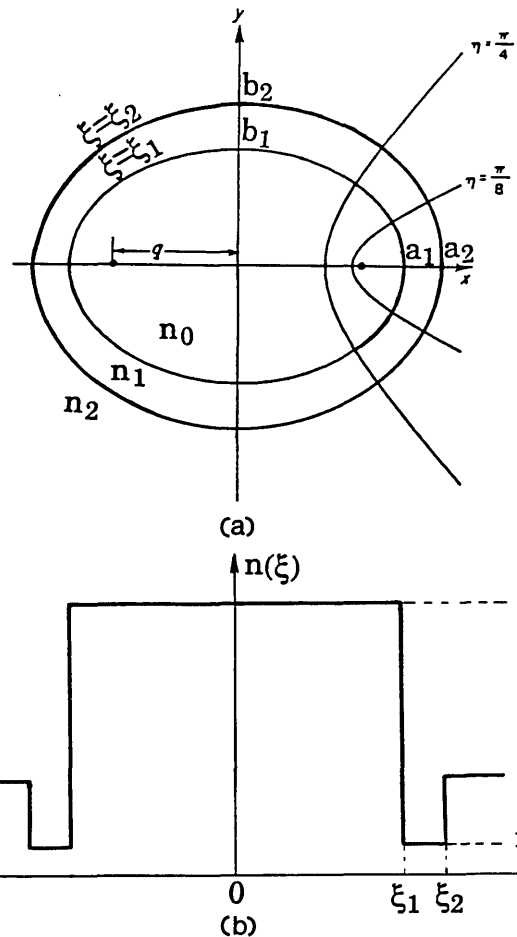

Fig. 1. (a) Schematic diagram of a double-clad elliptical fiber with depressed inner cladding. (b) Refractive index distribution in the radial direction.

Parameter $\Psi(x,y)$ is the scalar wave equation solution which has the scalar propagation constant β, i.e.,

$$[\nabla_t^2 + k^2 n^2(x,y) - \beta^2]\Psi(x,y) = 0, \tag{9}$$

where k is the wave number in vacuum and ∇_t is the transverse gradient operator. Parameters $\delta\beta_x$ and $\delta\beta_y$ are the polarization corrections resulting from the waveguide structure, which are given by[20]

$$\delta\beta_p = \frac{\rho_p(2\Delta_2)^{3/2}}{2V_p} \frac{\int_{-\infty}^{\infty}\int_{-\infty}^{\infty}(\nabla_t \cdot \mathbf{e}_t)\mathbf{e}_t \cdot \nabla f(x,y)dxdy}{\int_{-\infty}^{\infty}\int_{-\infty}^{\infty}\mathbf{e}_t^2 dxdy}, \quad p = x,y, \tag{10}$$

with $\rho_x = a_1$, $\rho_y = b_1$, and $\mathbf{e}_t = E_x\mathbf{i} + E_y\mathbf{j}$. As in the case of a SCE fiber, we approximate the fundamental mode of a DICE fiber by a 2-D Gaussian function[16,20]:

$$\Psi(x,y) = \exp\left[-\frac{1}{2}\left(\frac{X^2}{W_x^2} + \frac{Y^2}{W_y^2}\right)\right], \tag{11}$$

where $X = x/a_1$ and $Y = y/b_1$ and W_x, W_y are the normalized spot sizes,[21] which are the variational parameters to be determined along the major and minor

axes. The variational expression for the propagation constant β given by Eq. (9) can be written as[20]

$$\beta^2 = \frac{\int_{-\infty}^{\infty}\int_{-\infty}^{\infty}\left[k^2 n^2(X,Y)\Psi - \left(\frac{\partial\Psi}{\partial X}\right)^2 - \left(\frac{\partial\Psi}{\partial Y}\right)^2\right]dXdY}{\int_{-\infty}^{\infty}\int_{-\infty}^{\infty}\Psi^2 dXdY}. \tag{12}$$

The extremum equations,

$$\frac{\partial\beta}{\partial W_x} = 0, \quad \frac{\partial\beta}{\partial W_y} = 0, \tag{13}$$

lead to the spot size equations,[20]

$$\frac{\pi}{V_x^2} = \frac{W_x}{W_y}\int_{-\infty}^{\infty}\int_{-\infty}^{\infty} X\frac{\partial f}{\partial X}\exp\left(-\frac{X^2}{W_x^2} - \frac{Y^2}{W_y^2}\right)dXdY, \tag{14}$$

$$\frac{\pi}{V_y^2} = \frac{W_y}{W_x}\int_{-\infty}^{\infty}\int_{-\infty}^{\infty} Y\frac{\partial f}{\partial Y}\exp\left(-\frac{X^2}{W_x^2} - \frac{Y^2}{W_y^2}\right)dXdY. \tag{15}$$

Changing the coordinates X and Y in Eqs. (14) and (15) to elliptical coordinates ξ and η,

$$X = Q_x \cosh\xi \cos\eta, \tag{16}$$

$$Y = Q_y \sinh\xi \sin\eta, \tag{17}$$

with $Q_x = q/a_1$ and $Q_y = q/b_1$, we may obtain the spot size equations in the elliptical coordinates,

$$\frac{W_y}{W_x V_x^2} + \frac{W_x}{W_y V_y^2} = 2\int_0^\infty Q_x \cosh\xi Q_y \sinh\xi \frac{\partial f}{\partial \xi}\exp[-A(\xi)]I_0[B(\xi)]d\xi, \tag{18}$$

$$\frac{W_y}{W_x V_x^2} - \frac{W_x}{W_y V_y^2} = 2\int_0^\infty Q_x \cosh\xi Q_y \sinh\xi \frac{\partial f}{\partial \xi}\exp[-A(\xi)]I_1[B(\xi)]d\xi, \tag{19}$$

where $I_0(x)$ and $I_1(x)$ are modified Bessel functions of the first kind and of orders 0 and 1, respectively, and

$$A(\xi) = \frac{W_x^2 Q_y^2 \sinh^2\xi + W_y^2 Q_x^2 \cosh^2\xi}{2W_x^2 W_y^2},$$

$$B(\xi) = \frac{W_x^2 Q_y^2 \sinh^2\xi - W_y^2 Q_x^2 \cosh^2\xi}{2W_x^2 W_y^2}.$$

These equations can be used for a weakly guiding elliptical fiber with any refractive index profile. For a double-clad elliptical step-index fiber, f is given by Eq. (2), so that substituting

$$\frac{\partial f}{\partial \xi} = \alpha\delta(\xi - \xi_1) + (1 - \alpha)\delta(\xi - \xi_2)$$

into Eqs. (18) and (19) the spot size equations of DICE fibers can be finally obtained

$$\frac{W_y}{W_x V_x^2} + \frac{W_x}{W_y V_y^2} = 2\{\alpha \exp[-A(\xi_1)]I_0[B(\xi_1)]$$
$$+ (1 - \alpha)R_x R_y \exp[-A(\xi_2)]I_0[B(\xi_2)]\}, \tag{20}$$

$$\frac{W_y}{W_x V_x^2} - \frac{W_x}{W_y V_y^2} = 2\{\alpha \exp[-A(\xi_1)]I_1[B(\xi_1)]$$
$$+ (1 - \alpha)R_x R_y \exp[-A(\xi_2)]I_1[B(\xi_2)]\}, \tag{21}$$

where

$$A(\xi_1) = \frac{W_x^2 + W_y^2}{2W_x^2 W_y^2}, \quad B(\xi_1) = \frac{W_x^2 - W_y^2}{2W_x^2 W_y^2},$$

$$A(\xi_2) = \frac{W_x^2 R_y^2 + W_y^2 R_x^2}{2W_x^2 W_y^2}, \quad B(\xi_2) = \frac{W_x^2 R_y^2 - W_y^2 R_x^2}{2W_x^2 W_y^2}.$$

After solving Eqs. (20) and (21) for W_x and W_y, the polarization corrections $\delta\beta_x$ and $\delta\beta_y$ may be obtained by substituting Eqs. (7), (8) and (11) into Eq. (10).

$$\delta\beta_x = -\frac{(2\Delta_2)^{3/2}}{2a_1 V_x^3 W_x^4}, \tag{22}$$

$$\delta\beta_y = -\frac{(2\Delta_2)^{3/2}}{2b_1 V_y^3 W_y^4}. \tag{23}$$

Then the normalized birefringence is given by

$$B = \frac{\delta\beta_x - \delta\beta_y}{k} = \frac{2n_0\Delta_2^2}{V_y^4}\left[\frac{1}{W_y^4} - \frac{1}{(a_1/b_1)^4 W_x^4}\right]. \tag{24}$$

The modal dispersion is given by

$$\Delta\tau = \frac{1}{c}\frac{d(\delta\beta_x - \delta\beta_y)}{dk} = \frac{2n_0\Delta_2^2}{c}\frac{d}{dV_y}\left\{\frac{1}{V_y^3}\left[\frac{1}{W_y^4} - \frac{1}{(a_1/b_1)^4 W_x^4}\right]\right\}. \tag{25}$$

The normalized intensity is given by

$$S = \frac{\Psi^2}{\int_{-\infty}^{\infty}\int_{-\infty}^{\infty}\Psi^2 dXdY}, \tag{26}$$

$$\bar{S} = A_{core}S = \frac{\exp\left[-\frac{1}{2}\left(\frac{X^2}{W_x^2} + \frac{Y^2}{W_y^2}\right)\right]}{W_x W_y}, \tag{27}$$

with $A_{core} = \pi a_1 b_1$ being the elliptical core area.

III. Results and Discussion

A. Spot Size and Intensity Distribution

Figures 2(a) and (b) show the spot sizes W_x and W_y as functions of V_y for single-clad and double-clad fibers with $a_1/b_1 = 1.5$ and 3.0. The results for the single-clad fibers are the same as the theoretical results obtained previously,[16] and agree well with experimental results.[22] When the fiber is given a second cladding, the spot size becomes smaller. This means that the intensity distribution is more confined to the fiber center when a depressed inner cladding is introduced (see Fig. 3). Consequently, losses in the claddings may be decreased. This also loosens the angular alignment requirement during splicing.

B. Birefringence

The case of a single-clad elliptical fiber was analyzed by matching the boundary conditions and by solving the eigenvalue problem with the help of Mathieu functions.[2] Figure 4 compares the results obtained by such a method with those obtained by our Gaussian approximation. Between $1.3 \leq V_y \leq 3$, which is the region of greatest interest when single-mode fibers are
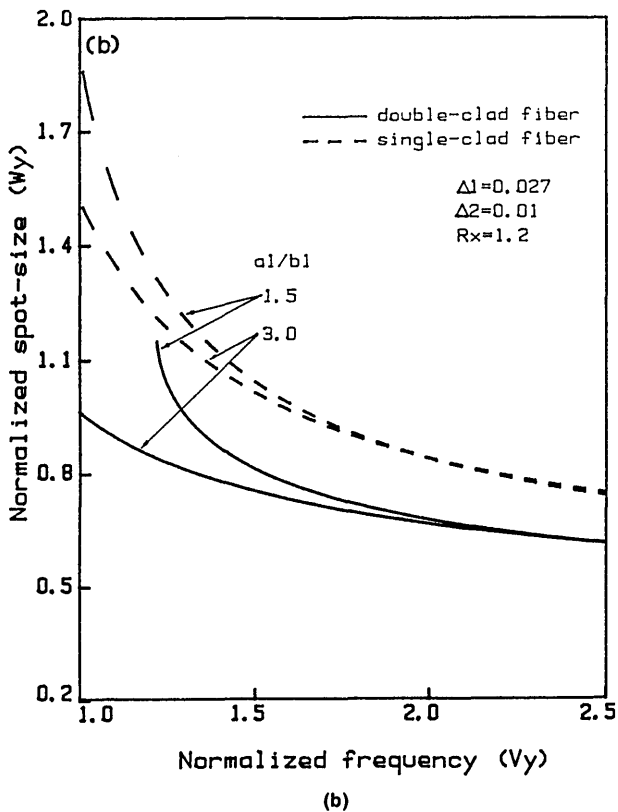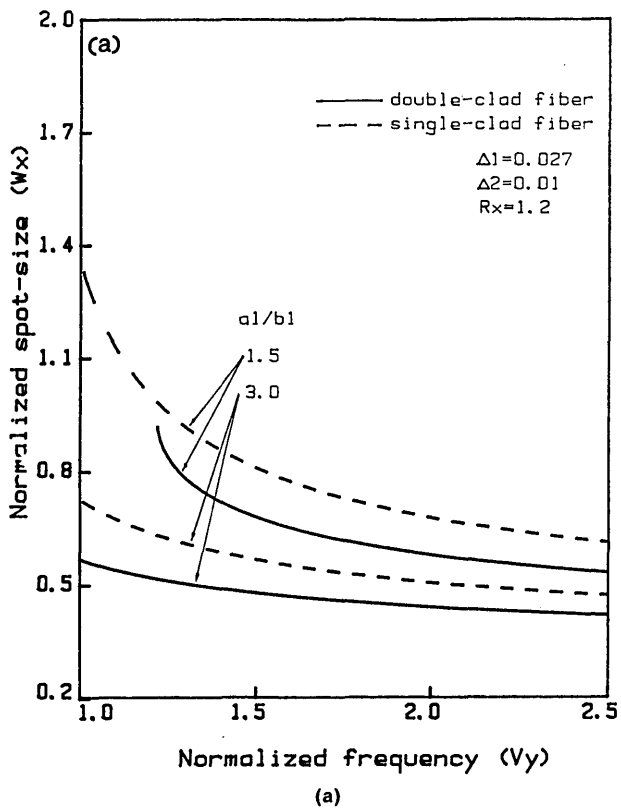
Fig. 2. (a) Spot size W_x vs V_y for a_1/b_1 = 1.5 and 3.0. (b) Spot-size W_y vs V_y for a_1/b_1 = 1.5 and 3.0. Solid and dashed lines correspond to double-clad and single-clad elliptical fibers, respectively.
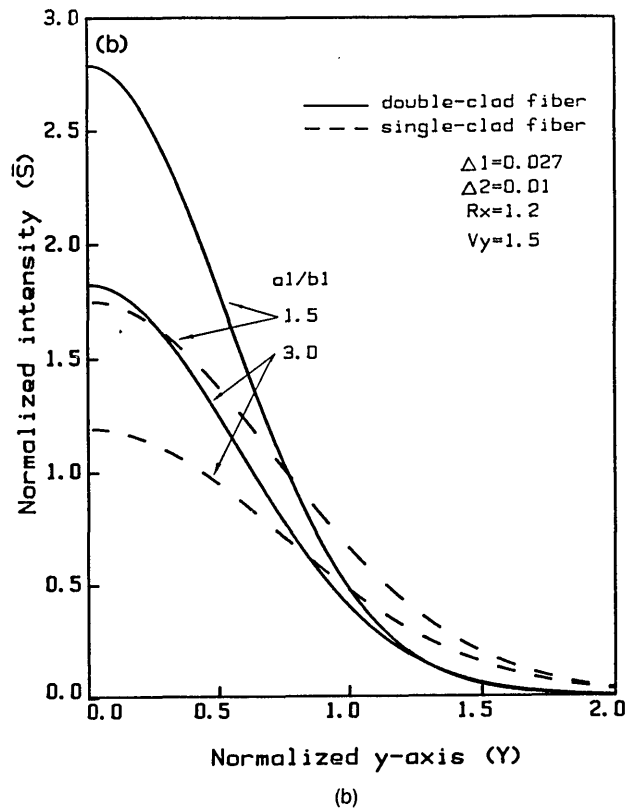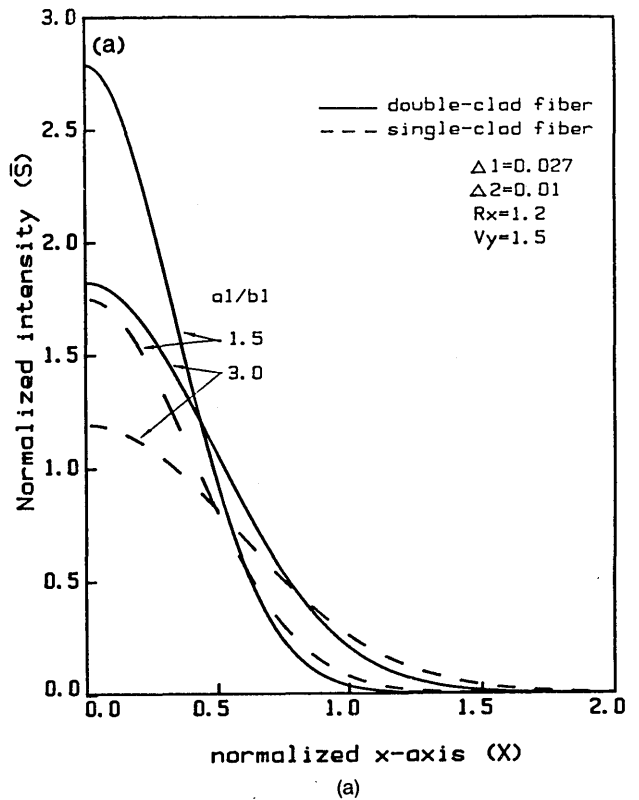

Fig. 3. (a) Intensity distributions along the minor axis. (b) Intensity distributions along the major axis. Solid and dashed lines correspond to double-clad and single-clad elliptical fibers, respectively.
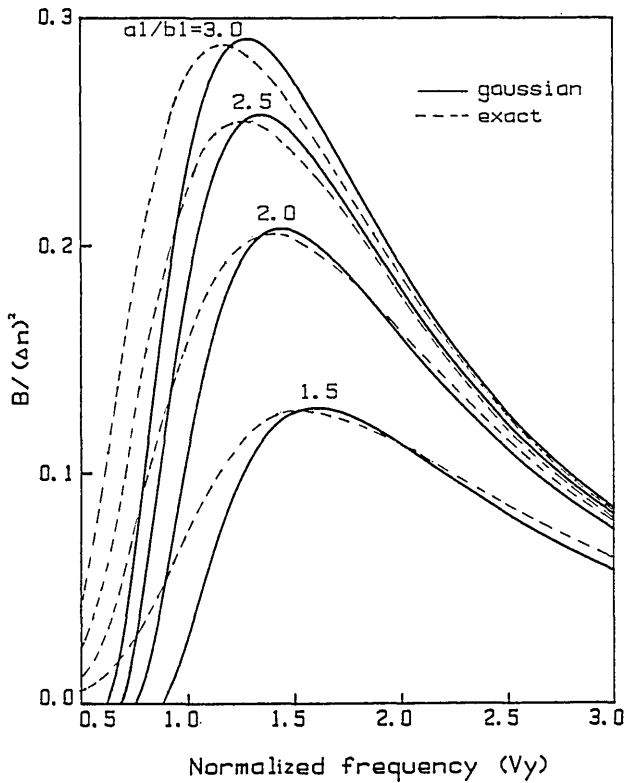
Fig. 4. Comparison between the birefringences obtained by the eigenvalue method using Mathieu's functions and the Gaussian approximation for a single-clad elliptical fiber.
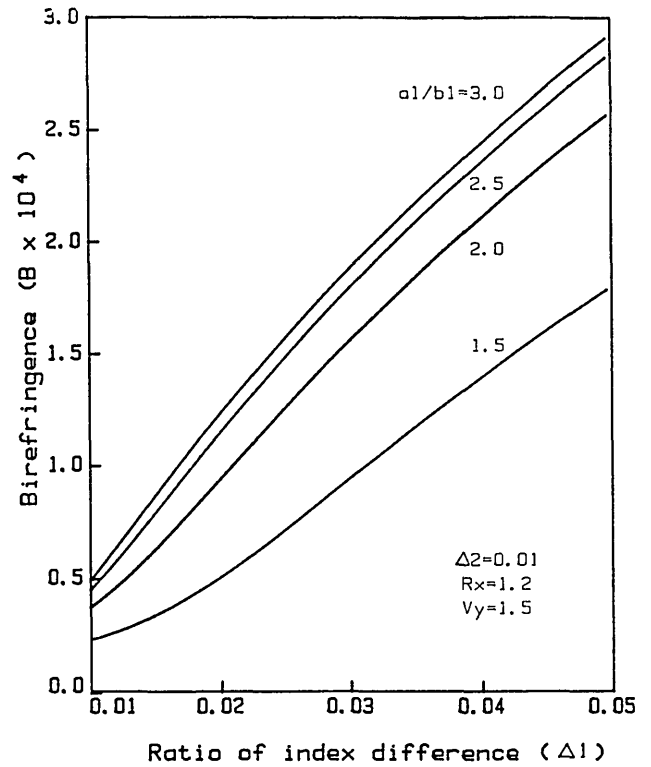

Fig. 6. Normalized birefringence B as a function of Δ_1 for $a_1/b_1 =$ 1.5, 2.0, 2.5, and 3.0.
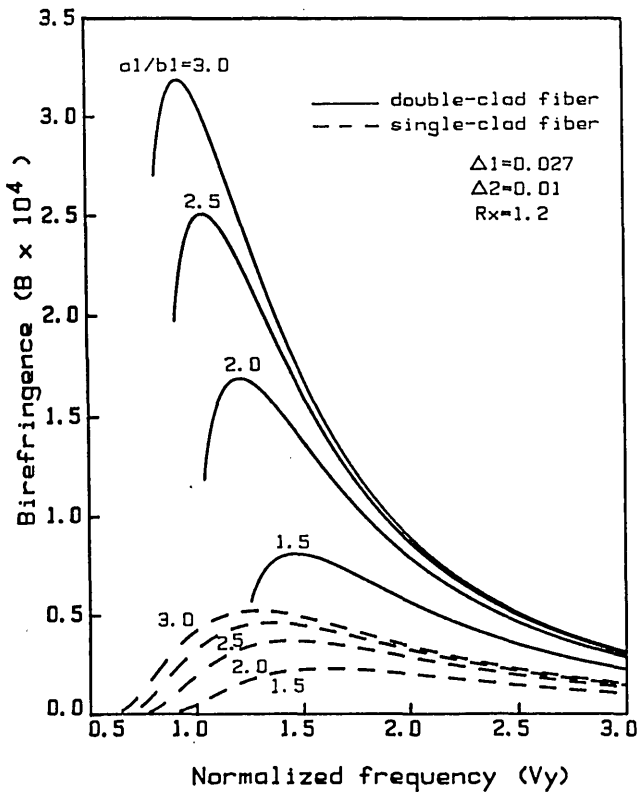

Fig. 5. Normalized birefringence B as a function of V_y for $a_1/b_1 =$ 1.5, 2.0, 2.5, and 3.0. Solid and dashed lines correspond to double-clad elliptical fibers and single-clad fibers.
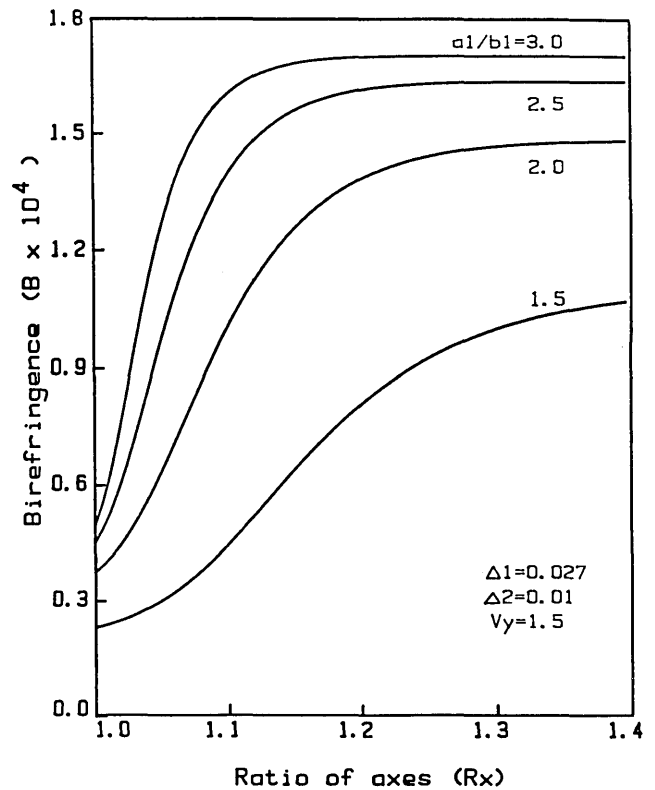

Fig. 7. Normalized birefringence B as a function of R_x for $a_1/b_1 =$ 1.5, 2.0, 2.5, and 3.0.

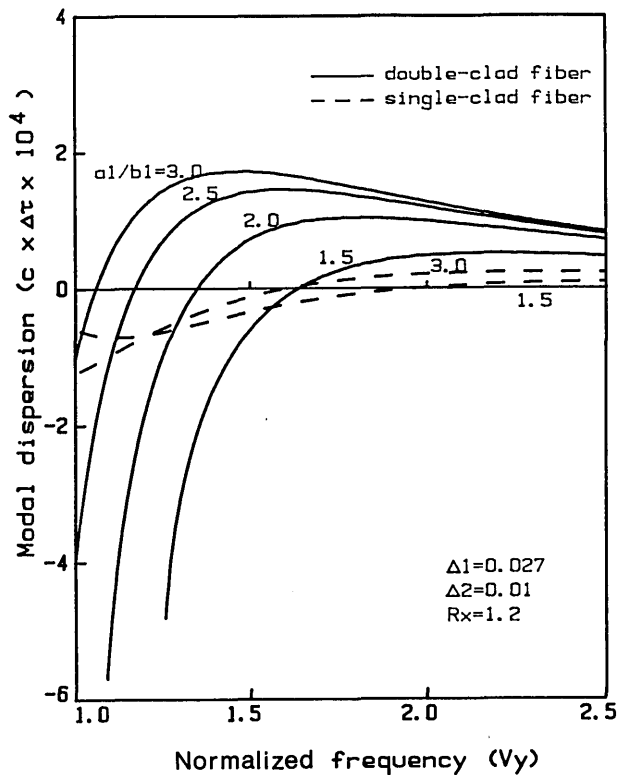5340   APPLIED OPTICS / Vol. 29, No. 36 / 20 December 1990

Fig. 8. Modal dispersion as a function of V_y for $a_1/b_1 = 1.5, 2.0, 2.5,$ and 3.0.
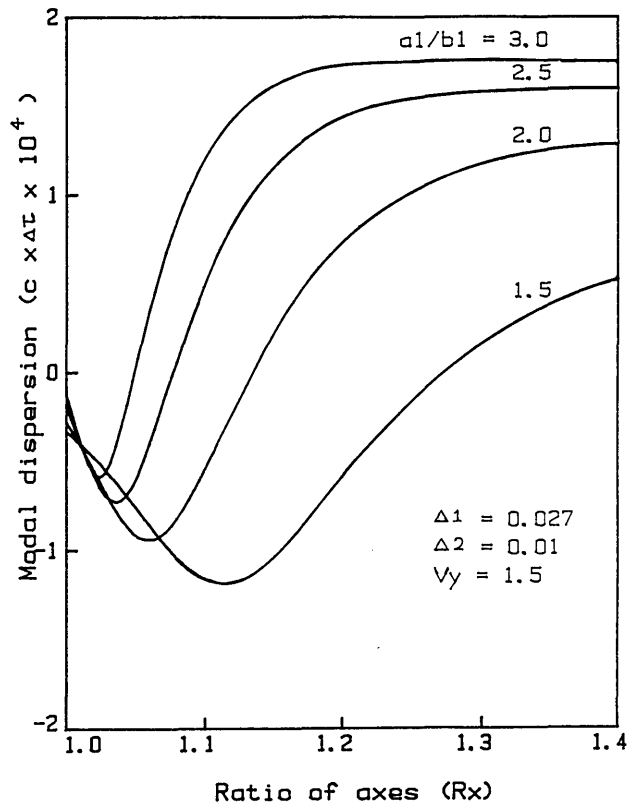

Fig. 10. Modal dispersion as a function of R_x for $a_1/b_1 = 1.5, 2.0, 2.5,$ and 3.0.
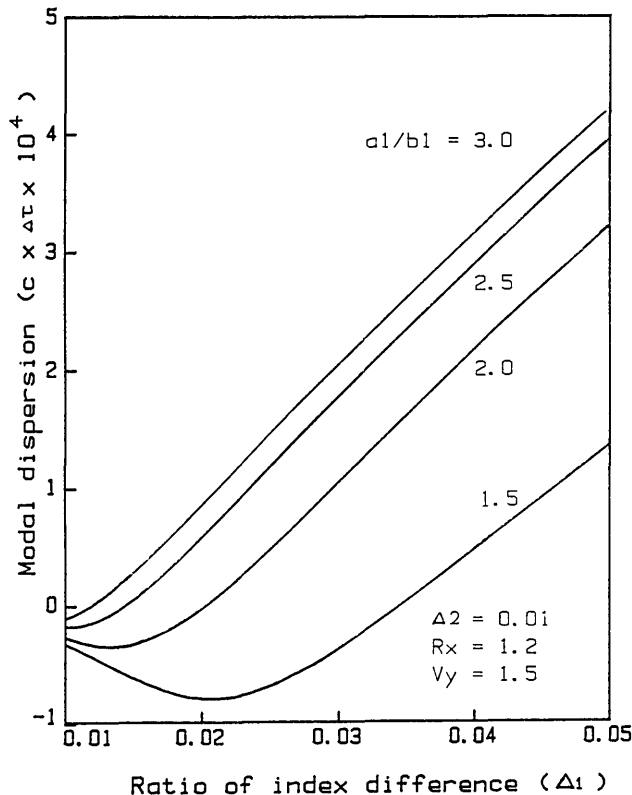

Fig. 9. Modal dispersion as a function of Δ_1 for $a_1/b_1 = 1.5, 2.0, 2.5,$ and 3.0.

used for information transmission, the two results agree well, with differences <8%.

Figure 5 shows the normalized birefringence B of DICE fibers as a function of V_y for $a_1/b_1 = 1.5, 2.0, 2.5,$ and 3.0. The maximum value of B for $a_1/b_1 = 3$ for a DICE fiber is ~6× as large as that for a SCE fiber.

Figure 6 shows B vs Δ_1 for $a_1/b_1 = 1.5, 2.0, 2.5,$ and 3.0. When $\Delta_1 = \Delta_2 = 0.01$, the fiber becomes a SCE fiber. The birefringence obviously increases with the refractive index difference Δ_1. This allows us to obtain high birefringence in weakly guiding DICE fibers by selecting Δ_1; such flexibility is not provided by SCE fibers.

Figure 7 shows B as a function of R_x, the ratio of the major axis of the core to that of the inner cladding for $a_1/b_1 = 1.5, 2.0, 2.5,$ and 3.0. When $R_x = 1$, the fiber is a SCE fiber; B increases sharply with R_x for $R_x < 1.3$, but changes little beyond $R_x = 1.4$.

C. Dispersion

Figure 8 shows the modal dispersion $c\Delta\tau$ as a function of V_y for $a_1/b_1 = 1.5, 2.0, 2.5,$ and 3.0. The zero dispersion points of DICE fibers occur at values of V_y smaller than those of SCE fibers. The more important fact is that all the cases shown in the figure fall within the single-mode operation range.[19]

Figures 9 and 10 give $c\Delta\tau$ as a function of Δ_1 and of R_x, respectively, for $a_1/b_1 = 1.5, 2.0, 2.5,$ and 3.0. Fig-

ures 8–10 show that the point at which a DICE fiber will have zero dispersion can be significantly shifted by adjusting the ratio a_1/b_1, index difference Δ_1, and ratio of axes R_x. This allows more flexibility in the design of high birefringence and dispersion free fibers.

IV. Conclusion

By using a scalar variational analysis based on Gaussian approximation of the fundamental mode, we have solved numerically the modal spot size equations for weakly guiding DICE fibers. We have presented the graphic results for the spot size, birefringence, and modal dispersion as functions of various important parameters, such as the normalized frequency V_y, the difference Δ_1 of the refractive index of the core and that of the inner cladding, and the ratio R_x of the inner cladding major axis to the core major axis. The field intensity distributions are also given. Moreover, fibers with different ellipticities a_1/b_1 are considered. We have shown that, when compared with a SCE fiber, a DICE fiber can give a smaller spot size, narrower field distribution, higher birefringence, and dispersion-free operation with smaller normalized frequencies.

References

1. C. Yeh, "Elliptical Dielectric Waveguides," J. Appl. Phys. **33**, 3235–3243 (1962).
2. R. B. Dyott, J. R. Cozens, and D. G. Morris, "Preservation of Polarization in Optical-Fiber Waveguides With Elliptical Cores," Electron. Lett. **15**, 380–382 (1979).
3. S. C. Rashleigh and M. J. Marrone, "Polarization Holding in Elliptical-Core Birefringent Fibers," IEEE J. Quantum Electron. **QE-18**, 1515–1523 (1982).
4. V. Ramaswamy, W. G. French, and R. D. Standley, "Polarization Characteristics of Noncircular Core Single-Mode Fibers," Appl. Opt. **17**, 3014–3017 (1978).
5. K. Kitayama, S. Seikai, N. Uchida, and M. Akiyama, "Polarization-Maintaining Single-Mode Fiber With Azimuthally Inhomogeneous Index Profile," Electron. Lett. **17**, 419–420 (1981).
6. T. Okoshi, K. Oyamada, M. Nishimura, and H. Yokota, "Side-Tunnel Fiber: An Approach to Polarization-Maintaining Optical Wave-Guiding Scheme," Electron. Lett. **18**, 824–826 (1982).
7. V. Ramaswamy, R. H. Stolen, M. D. Divine, and W. Plieble, "Birefringence in Elliptically Clad Borosilicate Single-Mode Fibers," Appl. Opt. **18**, 4080–4084 (1979).
8. S. C. Rashleigh and M. J. Marrone, "Polarization-Holding in a High-Birefringence Fiber," Electron. Lett. **18**, 326–327 (1982).
9. T. Hosaka, Y. Sasaki, J. Noda, and M. Horiguchi, "Low-Loss and Low-Crosstalk Polarization-Maintaining Optical Fibers," Electron. Lett. **21**, 920–921 (1985).
10. R. D. Birch, M. P. Varnham, D. N. Payne, and E. J. Tarbox, "Fabrication of Polarization-Maintaining Fibers Using Gas-Phase Etching," Electron Lett. **18**, 1036–1038 (1982).
11. R. H. Stolen, W. Pleibel, and J. R. Simpson, "High-Birefringence Optical Fibers by Preform Deformation," IEEE/OSA J. Lightwave Technol. **LT-2**, 639–641 (1984).
12. J. Noda, K. Okamoto, and Y. Sasaki, "Polarization-Maintaining Fibers and Their Applications," IEEE/OSA J. Lightwave Technol. **LT-4**, 1071–1089 (1986).
13. S. C. Rashleigh and M. J. Marrone, "Temperature Dependence of Stress Birefringence in an Elliptically Clad Fiber," Opt. Lett. **8**, 127–129 (1983).
14. A. N. Chester, S. Martellucci, and A. M. Verga Scheggi, "Optical Fiber Sensors," NATO ASI Series E: Appl. Sci. **132**, 18–19 (1987).
15. A. Kumar, R. K. Varshney, and K. Thyagarajan, "Birefringence Calculations in Elliptical-Core Optical Fibers," Electron. Lett. **20**, 112–113 (1984).
16. S. Sarkar, K. Thyagarajan, and A. Kumar, "Gaussian Approximation of the Fundamental Mode in Single Mode Elliptic Core Fibers," Opt. Commun. **49**, 178–183 (1984).
17. R. B. Dyott and J. Bello, "Self-Locating Elliptically Cored Fiber with an Accessible Guiding Region," Electron. Lett. **18**, 980–981 (1982).
18. R. K. Varshney, R. Srivastava, and R. V. Ramaswamy, "Characterization of Highly Elliptical Submicron Core Polarization Preserving Fibers: Theory and Experiment," Appl. Opt. **27**, 3114–3120 (1988).
19. R. K. Varshney and A. Kumar, "Effect of Depressed Inner Cladding on the Polarization Characteristics of Elliptical-Core Fibers," Opt. Lett. **9**, 522–525 (1984).
20. A. W. Snyder and J. D. Love, *Optical Waveguide Theory* (Chapman & Hall, London, 1983).
21. More than eight definitions have been proposed for spot size, and no agreement has been reached for a universally accepted one [E.-G. Neumann, *Single-Mode Fibers* (Springer-Verlag, New York, 1988), pp. 221–229.] The definition we used here is essentially that proposed by Snyder, "Understanding Monomode Optical Fibers," Proc. IEEE **69**, 6–12 (1981).
22. R. Yamauchi, T. Murayama, Y. Kikuchi, Y. Sugawara, and K. Inada, "Spot Sizes of Single-Mode Fibers with a Non-Circular Core," in *Technical Digest, Fourth International Conference on Integrated Optics and Optical Fiber Communication,* Tokyo (June 1983), 40–41.